

Optimal Hedging on Jump-diffusion Processes: Theory and Backtest

Yin Hei Chow¹

August 12, 2025

Submitted as coursework for The Certificate
in Quantitative Finance

¹Undergraduate, Department of Mathematics and Department of Physics, The University of Hong Kong,
Pokfulam Road, Hong Kong SAR (chowyh@connect.hku.hk)

Contents

1	Introduction	2
2	Mathematical background	3
2.1	Delta-hedging and Black-Scholes model	3
2.1.0.1	Delta-hedging and problem setting	4
2.2	Part 1 Volatility arbitrages	4
2.2.1	Merton's jump-diffusion model	4
2.2.1.1	Hedging the jump-diffusion	4
2.2.2	Hedging with implied volatility	5
2.2.2.1	Analytical profit and loss	5
2.2.3	Hedging with actual volatility	6
2.2.3.1	Analytical profit and loss	6
2.3	Part 2 Backtest of minimum variance delta-hedging	6
2.3.1	Problem setting and assumptions	6
2.3.2	Formulation of the optimization problem	7
3	Methodology	8
3.1	Part 1 Volatility arbitrages	8
3.1.1	Sobol sequence	8
3.2	Part 2 Backtest of minimum variance delta-hedging	10
3.2.1	Calibration of implied volatility surface and option greeks	10
3.2.1.1	Term rates from interpolating US treasury yields	10
3.2.1.2	Option-implied dividend yields	10
3.2.1.3	Market microstructure noise	11
4	Results and discussion	13
4.1	Part 1 Volatility arbitrages	13
4.1.1	Comparison between lognormal and jump-diffusion process	13
4.1.1.1	Future directions	14
4.1.2	Comparison of mark-to-market profits and expected shortfalls	14
4.1.2.1	Future directions	14
4.1.3	Characterization of profits with second order greeks	17
4.1.3.1	Favourable scenarios for Delta imp and Delta act hedging are exactly opposite	17
4.2	Part 2 Backtest of minimum variance delta-hedging	20
4.2.1	Stability and robustness	20
4.2.2	Further validation	21
4.2.2.1	Agreement with implied volatility surface	21
4.2.3	Limitations and future directions	25
5	Conclusion	26
6	Appendix	27

Chapter 1

Introduction

Delta-hedging is a foundational concepts in quantitative finance. Under the risk-neutral framework, it serves as the basis for no-arbitrage pricing of financial derivatives. In real-world markets, it is applied for both risk management and speculation. It is, however, known that directly hedging with Black-Scholes' delta tend to overhedge OTM and ITM options, while underhedging ATM option. Hull and White proposed an empirical model [1] for estimating the expected change in implied volatility as the underlying evolves, and the information can be incorporated for optimization of hedging performance under the minimum-variance delta formulation.

This report consists of two parts. Part 1 investigates different hedging strategies for exploiting a volatility arbitrage - hedging with the implied volatility versus with the actual forward volatility. The strategies are simulated on both lognormal and Merton's jump-diffusion dynamics, and arbitrage profits are found to be slightly worse in the jump-diffusion model in all cases despite having incorporated proper adjustments to the risk-neutral drift. The mark-to-market profits are found to be dependent on the option greeks in perculiar ways.

Part 2 concerns with backtesting the minimum-variance delta-hedging on 7-years of option data on S&P 500 starting from Jan 2017. It starts with calibrating the implied volaility surface together with option-implied dividend yields over a 10-year period from the start of 2014. The hedging strategy is then executed under a rolling calibration and the performance across delta-maturity buckets are evaluated for both call and put options.

Numerical methods implemented includes: Monte Carlo simulation of lognormal and jump-diffusion dynamics using Milstein scheme with Sobol sequence for the diffusive component; Tracking of option prices and greeks with Black-Scholes or Merton formulae; Tracking of the mark-to-market profits and expected shortfall of hedging strategies; Calibration of option-implied dividend yields; Calibration of implied volatility surfaces; Rolling calibration of the expected change in implied volatility on S&P 500; Optimization and evaluation of the minimum-variance delta hedging strategy by buckets.

Chapter 2

Mathematical background

2.1 Delta-hedging and Black-Scholes model

The Black-Scholes model assumes the underlying process S_t follows a lognormal dynamics

$$dS_t = (r - q)S_t dt + \sigma S_t dW^Q$$

defined by the risk-free rate r , dividend yield q , volatility σ and a Wiener process in an equivalent martingale measure Q to the real-world measure P . For a derivative whose value is of the form $V_t = V(t, S_t)$, Itô's lemma gives the integral equation

$$dV_t = \frac{\partial V}{\partial t} dt + \frac{\partial V}{\partial S} dS_t + \frac{1}{2} \sigma^2 S_t^2 \frac{\partial^2 V}{\partial S^2} dt$$

, and we define Black-Scholes delta of V to be $\Delta_t = \frac{\partial V}{\partial S}(t, S_t)$.

Consider the case when $q = 0$. Since the underlying itself has unit Black-Scholes delta, the portfolio $\Pi_t = V_t - \Delta_t S_t$ consisted of shorting Δ_t unit of underlying per unit of the derivative is locally risk-free. This is due to the portfolio's delta being zero :

$$\frac{\partial}{\partial S} \Pi_t = \Delta_t - \Delta_t = 0$$

By invoking the no-arbitrage principle, the portfolio must grows as the risk-free rate, and the Black-Scholes pricing equation for V results:

$$\begin{aligned} \frac{d\Pi}{dt} &= r\Pi \\ \iff \frac{\partial V}{\partial t} + \frac{1}{2} \sigma^2 S_t^2 \frac{\partial^2 V}{\partial S^2} &= r(V_t - \frac{\partial V}{\partial S} S_t) \end{aligned}$$

Upon imposing sufficient contract-specific boundary and terminal conditions, the equation could be solved analytically or numerically to give the risk-neutral present value V_0 of the contract.

In the more general case when $q \neq 0$, one may consider continuously reinvesting dividends into the underlying position to obtain the process $e^{qt} S_t$ as the value of such a position with no cash flows. Then, there exists a self-financing portfolio of the form

$$\Pi_t = A_t(V_t - \Delta_t e^{qt} S_t)$$

for some A_t and Δ_t , which could again be made locally risk-free by imposing

$$\frac{\partial}{\partial S} \Pi_t = A_t(\frac{\partial V}{\partial S} - \Delta_t e^{qt}) = 0$$

2.1.0.1 Delta-hedging and problem setting

This process of replicating the delta exposure of a derivative, and to take opposite position in the replicated position to reduce overall portfolio risk is known as delta-hedging or delta-replication. It is a common technique used by sellers of derivatives, who profit by adding a profit margin into the price of the derivative, or by volatility arbitrageurs, who bet on their beliefs that derivatives in the market are mispriced. The value of delta Δ_t , also called the hedging strategy, need not be $\frac{\partial V}{\partial S}$ and it depends on the choice of model for the underlying dynamics as well as the objective of the hedge in absence of a perfect hedge. It sets the problem of optimal hedging and is the topic of this report.

2.2 Part 1 Volatility arbitrages

A volatility arbitrage is present when one has a confident forecast of the actual volatility being significantly different from the implied volatility available in the market. If the forward actual volatility is above the implied volatility, options in the market are underpriced, and an arbitrage profit could be collected by first buying the options, and then cancelling out the risk by selling a synthetic version of the option. The synthetic option, made by delta-replication with the underlying, pays a higher premium because the underlying have a higher volatility than implied.

The similar argument works in the case when the forward actual volatility goes below the implied. One sell the overpriced option to the market, and delta-hedge their risk by taking a short position in the underlying of size Δ_t .

The first part of this report study in detail how this volatility arbitrage is brought about by restricting to the case for call options and with the forward actual volatility realising above the implied. We will consider the case with no dividends, and study two hedging strategies on both Black-Scholes model and Merton's jump-diffusion model [2] of the underlying.

2.2.1 Merton's jump-diffusion model

We have previously defined the underlying process in terms of Black-Scholes' lognormal random walk. To account for the fat tails and discontinuous jumps in empirical equity prices, the Merton model incorporates a Poisson jump component and gives the following dynamics:

$$dS_t = (r - q - \lambda E^Q[J - 1])S_t dt + \sigma S_t dW_t^Q + (J - 1)S_t dq_t^Q$$

where J is a random variable describing jump size, q_t is a Poisson process with intensity λ .

2.2.1.1 Hedging the jump-diffusion

There're two ways to hedge the jump-diffusion process. One is to assume that risk in the jump component is diversifiable, and thus it suffices to simply adjust the risk-neutral drift and only hedge the diffusive component in pricing the option. For our purpose, a deterministic jump size is implemented because it is the minimally required to render perfect hedging impossible. In this special case, the vanilla option prices can be solved to be

$$V_t^{\text{Merton}} = \sum_{n=0}^{+\infty} \frac{[\lambda J(T-t)]^n}{n!} e^{-\lambda J(T-t)} f(t, S_t, \sigma, r - \lambda(J-1) + n \frac{\ln J}{T-t})$$

where f is the Black-Scholes pricing formula for the same option with arguments time, underlying price, volatility, risk-free rate. Formulae for the greeks take the similar form of a sum of jump-adjusted Black-Scholes values weight by the probability that there will be n jumps in $[0, T]$. These formulae are essential in obtaining the mark-to-market arbitrage profits when the underlying follows a jump-diffusion process.

The alternative is to consider minimum variance delta-hedging. Taking variance as a risk measure, it is an objective to be minimize by varing the hedge Δ_t^{MV} . That is,

$$\Delta_t^{MV} = \operatorname{argmin}_{\Delta} \operatorname{Var}[d(V_t - \Delta S_t)]$$

The latter is not pursue here, however, the concept of minimum variance delta-hedging takes central stage in Part 2 and is backtest against 10-year European call and put options on the S&P 500 to see its effectiveness in real-world settings when perfect hedges are not realistic.

2.2.2 Hedging with implied volatility

First, consider the non-self-financing hedged position $\Pi_t^{imp} = V_t - \Delta_t^{imp} S_t$, that is, at all times t , we have a portfolio with a long position on a call and a short position of Δ_t^{imp} unit of underlying. Here, Δ_t^{imp} refers to the Black-Scholes delta when inputting the implied volatility, or

$$\begin{aligned}\Delta_t^{imp} &= e^{-q(T-t)} S_t \Phi(d_1(\sigma^{imp})) \\ d_1(\sigma^{imp}) &= \frac{\ln(\frac{S_t}{k}) + (r - q + \frac{1}{2}(\sigma^{imp})^2)(T - t)}{\sigma^{imp} \sqrt{T - t}}\end{aligned}$$

where k and T are the strike and maturity specific to a call option, Φ is the standard normal cumulative distribution function.

2.2.2.1 Analytical profit and loss

The portfolio defined this way is not self-financing and incur a funding cost of $r\Pi_t dt$ over $[t, t + dt]$. The mark-to-market (MtM) profit and loss is then

$$\text{PnL}_t^{imp} = \Pi_t - e^{rt} \Pi_0 + \int_0^t e^{r(t-\tau)} dCF_\tau$$

where dCF_t is the cash flow out of the hedged position Π_t over $[t, t + dt]$. When S_t is Ito, applying Ito's lemma on V_t (line 3) and Black-Scholes equation for σ^{imp} (line 4) discussed previously give

$$\begin{aligned}d\text{PnL}_t^{imp} &= d\Pi_t - r\Pi_t dt \\ &= dV_t - \Delta_t^{imp} S_t - r\Pi_t dt \\ &= \frac{\partial V}{\partial t} dt + \frac{1}{2} \sigma^2 S_t^2 \frac{\partial^2 V}{\partial S^2} dt - r(V_t - \Delta_t^{imp} S_t) dt \\ &= \frac{1}{2} [\sigma^2 - (\sigma^{imp})^2] S_t^2 \frac{\partial^2 V}{\partial S^2} dt\end{aligned}$$

This is integrated to give the following expression for future value of total profit

$$\begin{aligned}\text{PnL}_T^{imp} &= \int_0^T e^{r(T-t)} d\text{PnL}_t^{imp} \\ &= \frac{1}{2} [\sigma^2 - (\sigma^{imp})^2] e^{rT} \int_0^T e^{-rt} S_t^2 \Gamma_t^{imp} dt \\ &\geq 0\end{aligned}$$

where implied gamma Γ_t^{imp} refers to the Black-Scholes gamma obtained by inputting the implied volatility into Black-Scholes framework

$$\Gamma_t^{imp} = \frac{e^{-q(T-t)}}{S_t \sqrt{T-t} \sigma^{imp}} \Phi'(d_1(\sigma_t^{imp}))$$

This is in contrast to the actual gamma, which is the gamma of the replicated option.

The profit is maximized if the underlying process can maintain a high level of gamma over time. This is realized by having the underlying fluctuating around the strike price for prolonged periods of time, especially near maturity.

2.2.3 Hedging with actual volatility

Use the superscript *act* to label the analogous prices and greeks of the replicated option V_t^{act} . Hedging with actual volatility means that the Black-Scholes delta is computed using the actual level of volatility instead of the implied as follows

$$\Delta_t^{act} = e^{q(T-t)} S_t \Phi(d_1(\sigma)) ,$$

and analogously for other greeks. Then, the hedged portfolio $\Pi_t^{act} = V_t - \Delta_t^{act} S_t \forall t$ is equivalent to buying the underpriced option from the market and then selling the synthetic option V_t^{act} to receive a (synthesized) option premium throughout the period of hedging, and this premium will be larger than the cost of buying the option from the market for option price is a monotonic increasing function of volatility.

2.2.3.1 Analytical profit and loss

A similar analysis on the mark-to-market profit is done for this strategy. No-arbitrage principle on the portfolio $V_t^{act} - \Delta_t^{act} S_t$ gives

$$dV_t^{act} - \Delta_t^{act} S_t = r(V_t^{act} - \Delta_t^{act} S_t) dt$$

With this, and applying an integrating factor of e^{rt} in the final line, one derives

$$\begin{aligned} d\text{PnL}_t^{act} &= d\Pi_t^{act} - r\Pi_t^{act} dt \\ &= dV_t - rV_t dt - \Delta_t^{act} dS_t + r\Delta_t^{act} S_t dt \\ &= dV_t - rV_t dt - dV_t^{act} + rV_t^{act} dt \\ &= e^{rt} d[e^{-rt}(V_t - V_t^{act})] \end{aligned}$$

This expression is readily integrated and gives a total arbitrage profit of

$$\begin{aligned} \text{PnL}_T^{act} &= \int_0^T e^{r(T-t)} d\text{PnL}_t^{act} dt \\ &= e^{rT} \int_0^T d(e^{-rt}(V_t - V_t^{act})) \\ &= e^{rT} (V_0^{act} - V_0) \end{aligned}$$

which is the future value of the difference in option premium of the synthetic option and the market option. Note that the upper bound of the integral vanishes in line 3 because the payoff functions of the two options are identical.

2.3 Part 2 Backtest of minimum variance delta-hedging

2.3.1 Problem setting and assumptions

Part 2 of the report concerns with minimum variance delta-hedging using an empirical model derived in [1]. The model fits a functional form for predicting the change in implied volatility, and

thereby incorporate a correction term on top of the delta-hedging directly with Black-Scholes delta Δ_t^{BS} .

Implied volatility is defined such that for an European call or put option V_t ,

$$V_t = f(t, S_t, \sigma_t^{imp}, r_t, q_t)$$

for some Black-Scholes pricing formula f that depends of the option type, strike k , and maturity date T . Take the assumption that both S_t and σ_t^{imp} are Ito processes, and that dividend yield and interest rate change slowly enough in comparison

$$dr_t, dq_t \sim O(dt) = O(dS_t^2)$$

Ito-Taylor expansion for the option price is then

$$dV_t = \frac{\partial V}{\partial S} dS_t + \frac{\partial V}{\partial \sigma_t^{imp}} d\sigma_t^{imp} + O(dS_t^2)$$

2.3.2 Formulation of the optimization problem

Hedging is the minimization of risk, and if variance of the hedged portfolio $\Pi_t = V_t - \Delta_t S_t$ is chosen to be the risk measure, the minimum variance delta is the hedging strategy Δ_t such that variance risk of the hedged portfolio is minimal, or

$$\Delta_t^{MV} = \operatorname{argmin}_{\Delta} \operatorname{Var}[d(\Pi_t)]$$

When implied volatility changes with the underlying, or when hedging the jump risk together with the diffusion risk in Merton model mentioned in Part 1, the optimal hedge is no longer the Black-Scholes delta Δ_t^{BS} . Let $dV_t, dS_t, d\sigma_t^{imp}$ all be forward differences in the below discretization, that is, $dV_t = V_{t+dt} - V_t$ for example. Let \mathcal{F}_t be all available information in the underlying and the option market up to time t , and \mathcal{G}_t denotes all available information in \mathcal{F}_t together with the knowledge of what dS_t is, but not about dV_t and hence $d\sigma_t^{imp}$. We now solves for Δ_t^{MV} . The first moment of hedging error

$$E[dV_t - \Delta_t^{MV} dS_t | \mathcal{G}_t] = \Delta_t^{BS} dS_t - \Delta_t^{MV} dS_t + v_t^{BS} E[d\sigma_t^{imp} | \mathcal{G}_t] + O(dt)$$

requires that

$$\Delta_t^{MV} = \Delta_t^{BS} + v_t^{BS} \frac{\partial E[\sigma_t^{imp} | \mathcal{G}_t]}{\partial S}$$

in order that $\Delta_t^{MV} dS_t$ be an unbiased estimator of the random variable dV_t as $dt \rightarrow 0$. Hull and White [1] found

$$\frac{\partial E[\sigma_t^{imp} | \mathcal{G}_t]}{\partial S} \approx \frac{a_t + b_t \Delta_t^{BS} + c_t (\Delta_t^{BS})^2}{S_t \sqrt{T-t}}$$

to be a good approximation empirically for S&P 500 option data. The remaining task is to minimize the second moment $E[(dV_t - \Delta_t^{MV} dS_t)^2 | \mathcal{G}_t]$, or equivalently the sum of square error (SSE), to fit (a,b,c) onto real data. The model was shown to out-perform more complicated model such as stochastic volatility model and Dupire's local volatility model, despite having significantly fewer degrees of freedom.

Chapter 3

Methodology

3.1 Part 1 Volatility arbitrages

A hypothetical setting with $r = 0.06$, $q = 0$, $T = 1$, $S_0 = 1$, $k = S_0 * 1.1$, $\sigma = 0.4$, $\sigma^{imp} = 0.2$ is used to test the two hedging strategies. The spot price S_0 is set to unit because that allow expressing the total profit in terms of a proportion of the initial net value of the position in underlying. When the Merton model is used instead, the above parameters are held unchange, but with $\lambda = 0.1$ and $J = 0.8$, which correspond to a 20% drop. The Black-Scholes model is recovered by setting $J = 1$ in the python implementation.

To obtain the mark-to-market profits, Milstein scheme with Sobol low discrepancy sequence is implemented to sample the diffusion component of the underlying process. That is, for a lognormal underlying,

$$S_{t+dt} = S_t + \mu S_t dt + \sigma S_t dW_t + \frac{1}{2} \sigma^2 S_t (dW_t^2 - dt)$$

where dt is a finite time step chosen to be about a quarter of a trading day.

3.1.1 Sobol sequence

A discretized asset path S_t is in the space $\mathbb{R}^{T/dt}$ where $\frac{T}{dt}$ is the number of time steps. To best represent the statistics of S_t with a fixed number of Monte Carlo samples, Sobol low discrepancy sequences can be used to fill a hypercube $[0, 1]^{T/dt}$ more uniformly than a truly random sequence. The Sobol sequence is deterministic quasi-random, a random scramble of the sequence in $\frac{T}{dt}$ dimension of length 2^{12} (which is the chosen number of Monte Carlo samples) is obtained before mapping them into a standard normal distribution to be used as the Wiener process increments dW_t . Note that the number of Monte Carlo samples has to be a power of 2 in order that the balance property be satisfied.

For Merton model, the same method is used to sample the diffusive component, and the Poisson process is sampled randomly [3]. The risk-neutral drift has to be adjusted by

$$\mu = r - q - \lambda E[J - 1]$$

to be comparable to the Black-Scholes model.

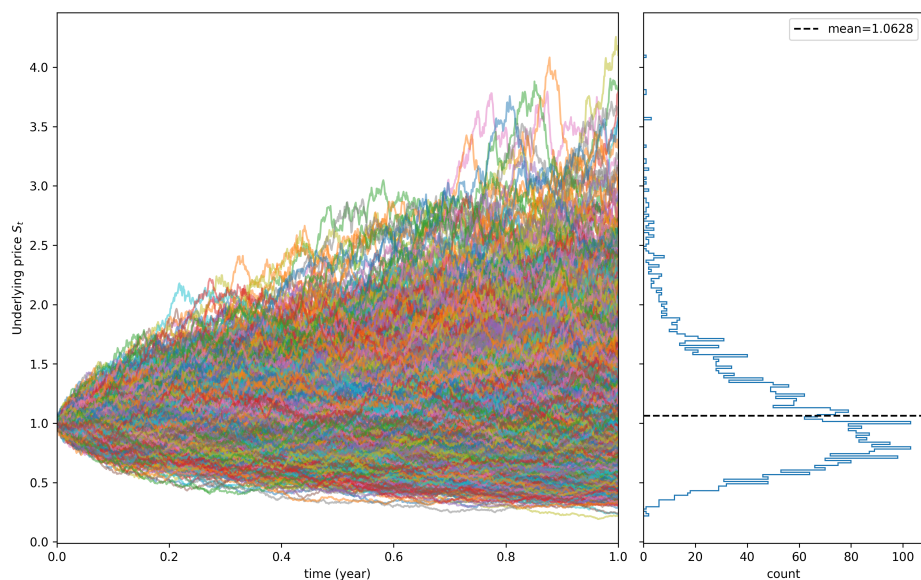


Figure 3.1: A Monte Carlo sampling of the lognormal underlying process S_t is shown in the main panel. Terminal values are aggregated into an empirical distribution in the right panel

3.2 Part 2 Backtest of minimum variance delta-hedging

The minimum variance delta-hedging strategy is tested on a matrix of moneyness-maturity buckets, or $(\Delta_t^{BS}, T - t)$ -bucket to be precise. The hedging gain defined as

$$\text{gain}_{[t,T]}(\Delta^{MV}) = 1 - \frac{\int_t^T (dV_\tau - \Delta_\tau^{MV} dS_\tau)^2}{\int_t^T (dV_\tau - \Delta_\tau^{BS} dS_\tau)^2}$$

is used as the performance metric for evaluating the effectiveness of the hedge relative to directly hedging with Δ_t^{BS} .

3.2.1 Calibration of implied volatility surface and option greeks

The minimum variance delta-hedging strategy is backtested on 7-year of option data on the S&P500 from Jan 2017 to Dec 2023. 10-year European call and put options data (SPX 500) starting from Jan 2014 is retrieved from OptionMetrics [4], which includes an extra 3-year period in front for the rolling estimation of the model parameters (a, b, c) . For each month starting from Jan 2017, the empirical model is fitted on the previous 3-year and then tested on that month. The calibration is done separately for each moneyness-maturity buckets, and separately for call and put options.

The data comes with fitted implied volatility surface and option greeks, but they are not used. Instead, all implied volatility and greeks are calibrated from first principle on the option prices with the following two time-series: interest rate and dividend yields.

3.2.1.1 Term rates from interpolating US treasury yields

For time-varying risk-free rate r_t , the option prices and greeks are obtained by inputting the time-averaged risk-free rate as the constant level of r in any Black-Scholes formulae. This is called the term rate $r(t, T)$ and it depends on the quote date and the maturity date. The US treasury rates is a good proxy for the risk-free rate since the underlying consists of stocks traded in the US market.

Term rates for all option maturities on all quote dates are obtained by linear interpolation of the US treasure yield curves available almost every trading day from the start of 2014 to the end fo 2023. Data on missing dates are forward-filled with the latest data, and the gap doesn't exceed 3 trading days or 4 calendar days.

3.2.1.2 Option-implied dividend yields

As an index, S&P 500 is non-tradable and pays dividends to no one. Its dividend yield need to be considered nonetheless to obtain the proper risk-neutral drift in pricing. The historical dividend yield is not used because that would incorporates future information into the backtest. Rather, the option-implied dividend yield [5, 6] is deduced solely from the option market as a forward-looking quantity as follows:

On each quote date t and for each maturity bucket, select all pairs of call and put whose strike k falls into a factor of two around the spot price. Assuming the no-arbitrage principle holds strongly as long as the options are not deeply OMT or IMT, we have the put-call parity

$$C(k) - P(k) = e^{-r(T-t)}(F_t - k)$$

and the relation

$$F_t = e^{q(T-t)}S_t$$

This allow solving for a value of $q(k, t, T)$ for each option pair uniquely labelled by (k, t, T) , and the option-implied dividend yield is obtained as the median across strikes

$$q(t, T) = \text{median}\{q(k, t, T) : 0.5 \leq \frac{k}{S_t} \leq 2\}$$

3.2.1.3 Market microstructure noise

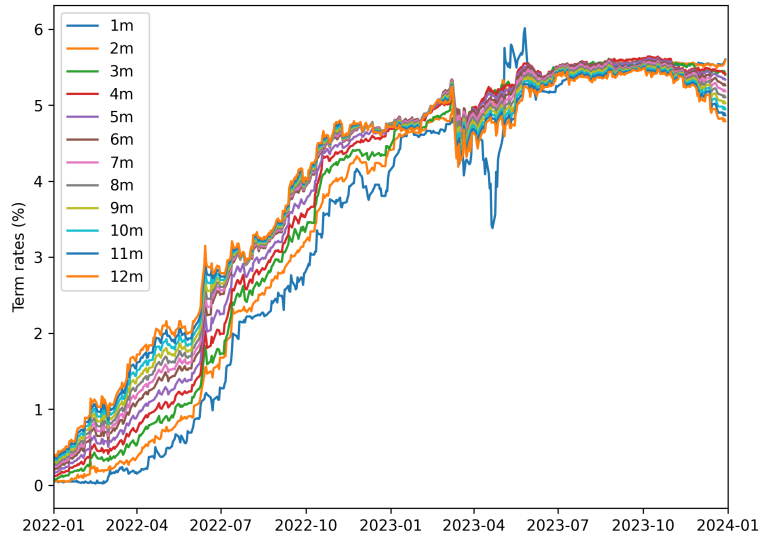


Figure 3.2: Term rates interpolated from daily US treasure yield curves. The figure spans from Jan 2014 to Dec 2023, but only term rates over the final year of monthly maturities are displayed here for a clean illustration.

The fitted implied volatility surface (3.4) is rough for near-maturity deeply ITM call and put options. This is due to low trading volume and wide bid-ask spreads. Those noise get amplified near maturity where vega shrinks to zero, and therefore, implied volatility has a high sensitivity on changes in option price. To address this, options with delta below 0.05 and above 0.95 are discarded from the dataset.

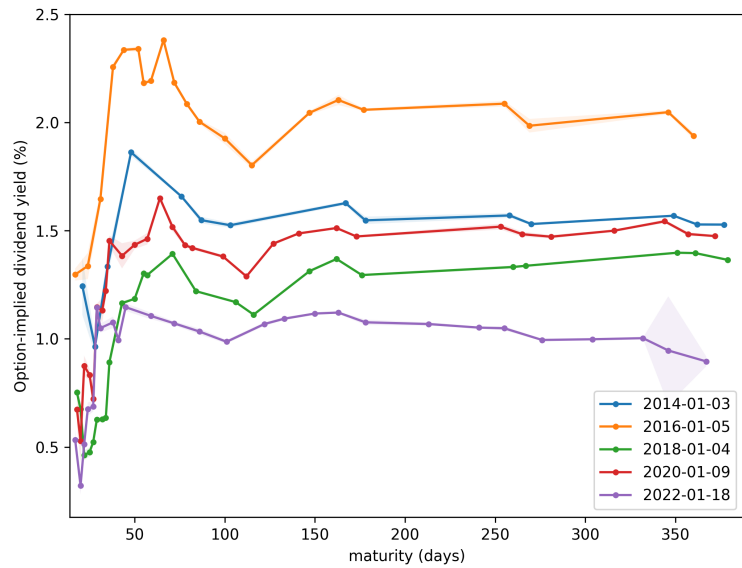
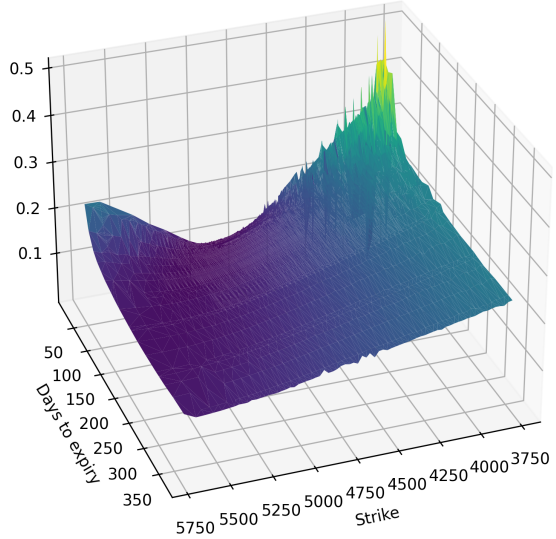


Figure 3.3: Option-implied dividend yield curves on different quote dates

Call-implied volatility surface on 2023-12-29



Put-implied volatility surface on 2023-12-29

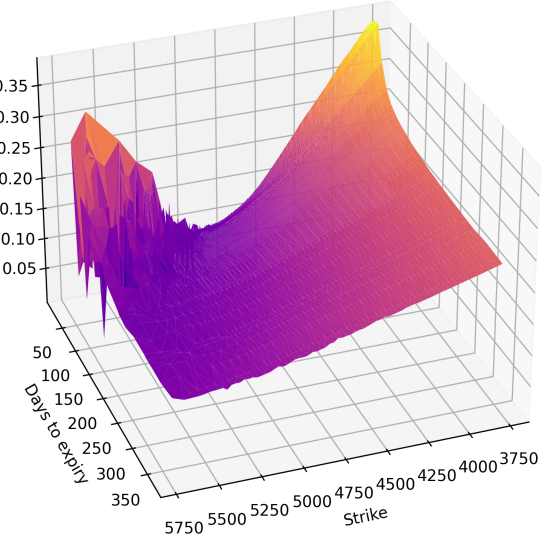


Figure 3.4: Implied volatility surface fitted on call and put options on a particular day. The surface is rough for both closed to maturity deeply ITM and put options.

Chapter 4

Results and discussion

4.1 Part 1 Volatility arbitrages

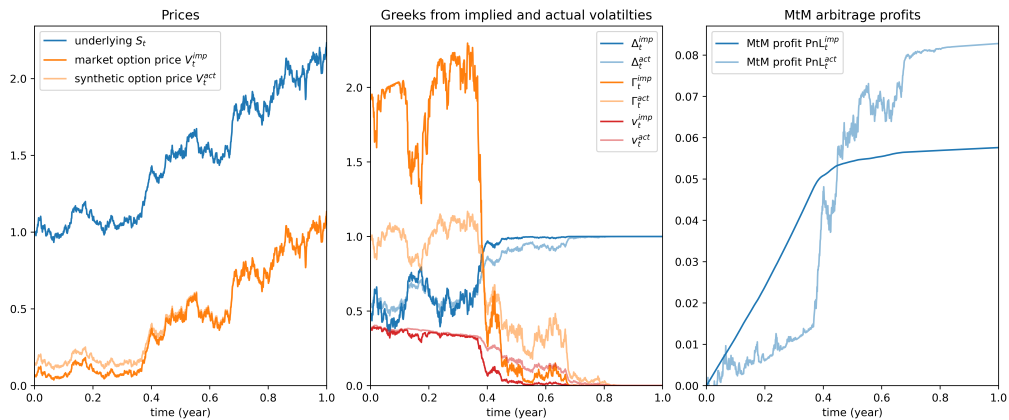


Figure 4.1: Merton’s jump-diffusion framework for the underlying, option price and greeks. The right panel shows the mark-to-market profits for hedging with implied and with actual volatility.

Figure 4.1 depicts a typical output of the Monte Carlo simulation. It tracks the option prices and greeks output by inputting the two volatilities into Merton’s formulae, and the mark-to-market profits for both strategies are computed.

Underlying dynamics	Hedging strategy	Expected profit (%)	Expected shortfall (%) at 95% c.l.	Support
lognormal	Δ_t^{imp}	8.43	1.47	2^{12}
	Δ_t^{act}	8.45	8.32	2^{12}
jump-diffusion	Δ_t^{imp}	8.30	1.55	2^{12}
	Δ_t^{act}	8.27	8.17	2^{12}

Table 4.1: Summary on arbitrage profits in the two hedging strategies.

4.1.1 Comparison between lognormal and jump-diffusion process

Table 4.1 reports the arbitrage mean profits and expected shortfalls. The convention taken for expected shortfall is the expected profit conditioned on the fact that the profit is in the bottom 5%

of profits, but not the negative of this value. The expected profits are in good agreement to their respective analytical values derived in chapter two.

The mean profits on the jump-diffusion process is slightly worse than on lognormal regardless of which hedging strategy is employed, despite having adjusted the risk-neutral drift by

$$\mu = r - q - \lambda E[J - 1]$$

The expected shortfall at 95% confidence level is also worse on jump-diffusion than on the lognormal process for hedging with actual volatility. This is because discontinuities fundamentally cannot be hedged, and having jumps introduce hedging errors that chip away at the arbitrage profits.

It is strange that the expected shortfall is better in jump-diffusion than in lognormal process for Δ_t^{imp} , which doesn't fit the pattern. However, looking at the entire profit distribution 4.2a, the distribution may not be regular enough at this number of Monte Carlo samples to give an accurate measurement of tail statistics.

4.1.1.1 Future directions

The hedging of jump-diffusion by hedging only the diffusion component has the limitation that it assumes jump risks to be priced in [2]. Further investigation can be done by hedging using the minimum-variance delta that hedge both the jump and diffusion components. It will be interesting to see if the mean profit is improved or made worse.

4.1.2 Comparison of mark-to-market profits and expected shortfalls

Findings in this section and the next section applies for both lognormal and jump-diffusion processes, and only the figures for the former is shown for brevity. For a typical sample path of MtM profits under a jump-diffusion process, see figure 4.1.

The total profits in hedging with implied volatility is random, as reflected by the distribution figure 4.2a, with a mean close to the deterministic profits in hedging with actual volatility 4.2b. This close agreement in mean values is found to be true also for the mark-to-market profits, depicted in the right panel of figure 4.3. Mark-to-market profits of Δ_t^{imp} are monotonically increasing, which is guaranteed by

$$dPnL_t^{imp} = \frac{1}{2}[\sigma^2 - (\sigma^{imp})^2]S_t^2\Gamma_t^{imp}dt \geq 0$$

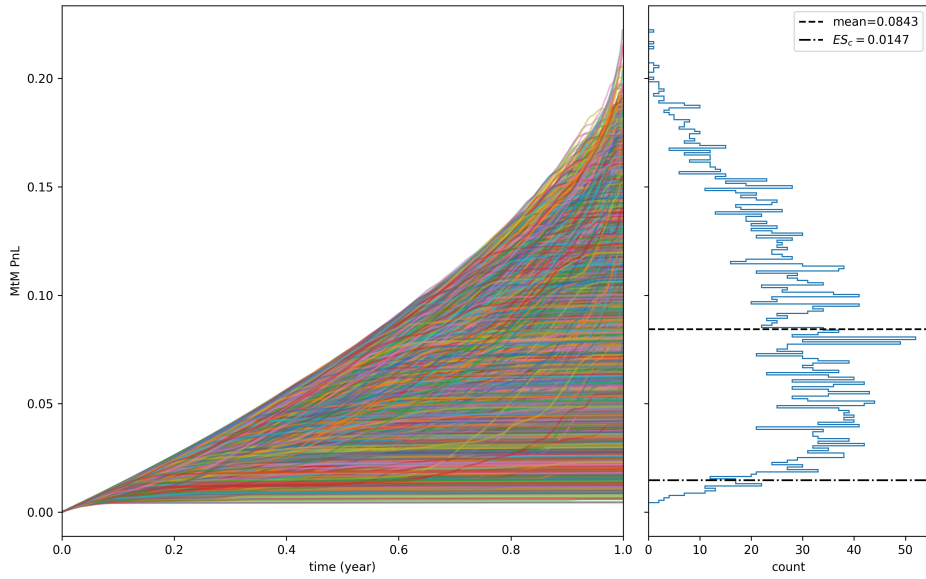
for options whose gamma doesn't change sign. In contrast, that for Δ_t^{act} has large drawdowns and underwater time, which appears to imply that the strategy is less preferable on first sight.

The expected shortfall converges to the mean for Δ_t^{act} as the number of Monte Carlo samples increases. The profit distribution for Δ_t^{imp} exhibit a positive skew but has a much worse expected shortfall. If one views the expected shortfall of the MtM profits 4.3, that for Δ_t^{act} starts off worse than Δ_t^{imp} for about one-third of the option lifetime, but maintains substantially better than Δ_t^{imp} in the remaining time.

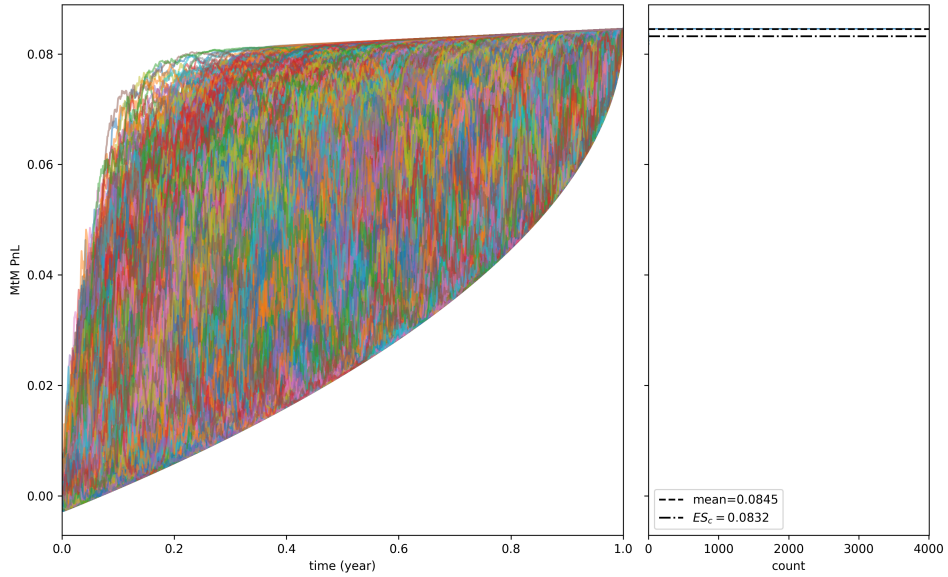
It is therefore tempting to make the conclusion that no one strategy is better and it comes down to individual risk preferences. Still, it is worth investigating under what scenarios could the highest returns in Δ_t^{imp} hedging be obtained, which motivates the following section.

4.1.2.1 Future directions

The rolling Sharpe ratio and Calmar ratio could be calculated to provide quantitative statements about the risk-returns trade-off MtM.



(a) Hedged with implied volatility



(b) Hedged with actual volatility

Figure 4.2: Shown in the main panels are Monte Carlo samples of the mark-to-market profit of the two hedging strategies. Terminal values are aggregated to form the distributions in the right panels, which contain also information of the expected profits and the expected shortfall at 95% confidence level.

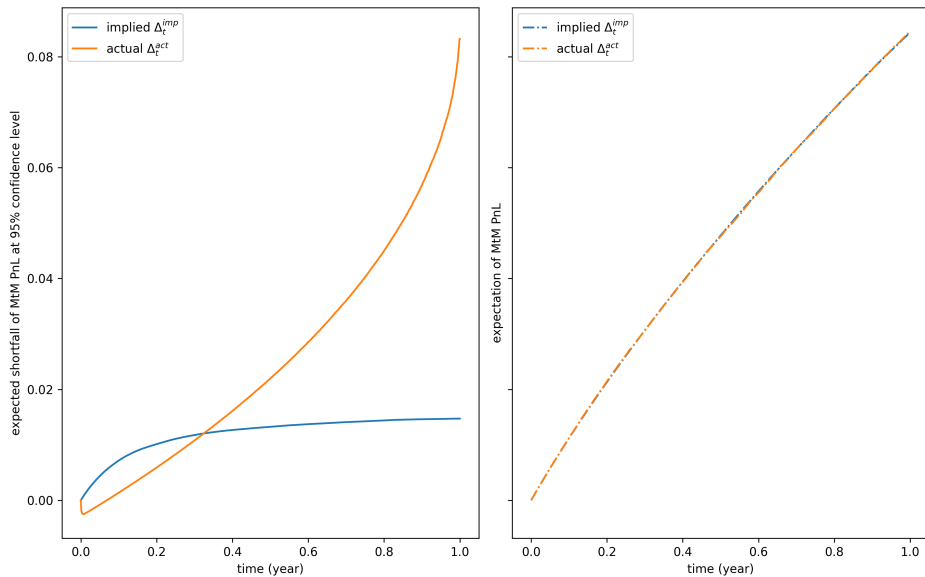


Figure 4.3: Expected shortfalls and expectations of the mark-to-market profits of hedging strategies Δ_t^{imp} and Δ_t^{act} .

4.1.3 Characterization of profits with second order greeks

It is observed that the random profits of implied volatility hedging Δ_t^{imp} are the lowest (around 0.004 to 0.013) for realized asset paths that have the fastest-decaying Black-Scholes vega v_t^{imp} (figure 4.4a). On the contrary, these profits are the largest (around 0.13 to 0.175) on paths with the slowest-decaying vega (figure ??). To quantify this relation, figure 4.5a plots the linear relation between total profits PnL_T^{imp} against quadratic variations of vega, and the variables have a Pearson correlation of 0.7299 on a lognormal process, and 0.7033 on a jump-diffusion process.

The quadratic variation of vega, defined as $\int_0^T (dv_t^{imp})^2$, is found to be a good proxy for quantifying whether the quantity is fast-decaying. This is because vega in this case is bounded below, and a fast-decaying vega has its fluctuations largely scaled down for most of the option lifetime.

This implied vega v_t^{imp} measures the sensitivity of the market option on the implied volatility. Results suggest that by hedging with the implied volatility, the profit is generally larger if the market option could maintain a high level of sensitivity on this implied volatility for a longer periods of time.

This could be explained from the expression

$$PnL_T^{imp} = \frac{1}{2} [\sigma^2 - (\sigma^{imp})^2] e^{rT} \int_0^T e^{-rt} S_t^2 \Gamma_t^{imp} dt$$

Black-Scholes vega takes the form

$$v_t^{imp} = e^{-q(T-t)} S_t \sqrt{T-t} \Phi'(d_1(\sigma^{imp}))$$

while gamma takes the form

$$\Gamma_t^{imp} = \frac{e^{-q(T-t)}}{S \sqrt{T-t} \sigma^{imp}} \Phi'(d_1(\sigma^{imp}))$$

Vega is high precisely when the option is near ATM, which is also when gamma is high. Gamma also gets especially large if the option can be maintained near ATM close to maturity, due to the singularity $\frac{1}{\sqrt{T-t}}$. A path with a large gamma for prolonged periods of time will then integrate to a larger PnL_T^{imp} .

4.1.3.1 Favourable scenarios for Δ_t^{imp} and Δ_t^{act} hedging are exactly opposite

For the case of Δ_t^{act} , the total profit is fixed but how it is brought about depends on S_t . Figure 4.6 shows the MtM profit for Δ_t^{act} for fast-decaying gamma and diverging gamma scenarios. Note that these two scenarios are exactly the above cases where vega is fast-decaying versus slow-decaying. It is observed that the MtM profit has smaller drawdowns when gamma is fast-decaying. Most profits are also made early, which is favourable.

The conclusion can therefore be drawn that if one forecasts the actual volatility to be away from the implied, and forecasts that the underlying will remain close to the strike price over long periods of time until maturity, hedging with implied volatility is likely to be more profitable than hedging with actual volatility - all while avoiding drawdown periods throughout.

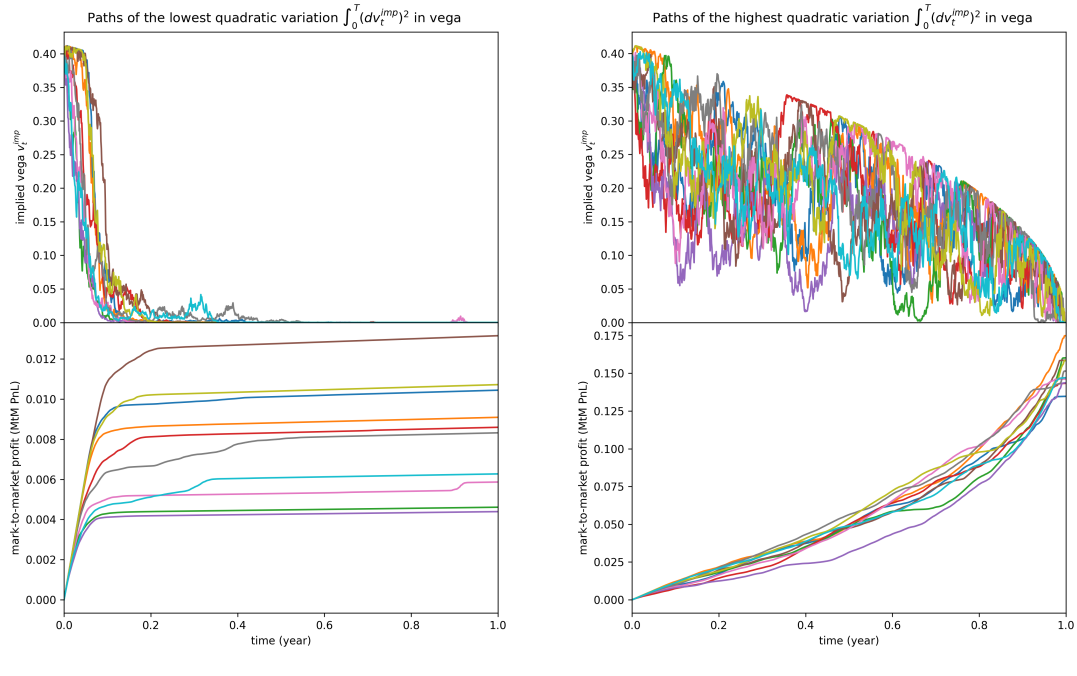


Figure 4.4: Case studies. Comparison of the mark-to-market profits of the hedging strategy Δ_t^{imp} with implied volatility in the scenarios when (a) asset paths have fast-decaying vegas; versus (b) when asset paths have slow-decaying vegas.

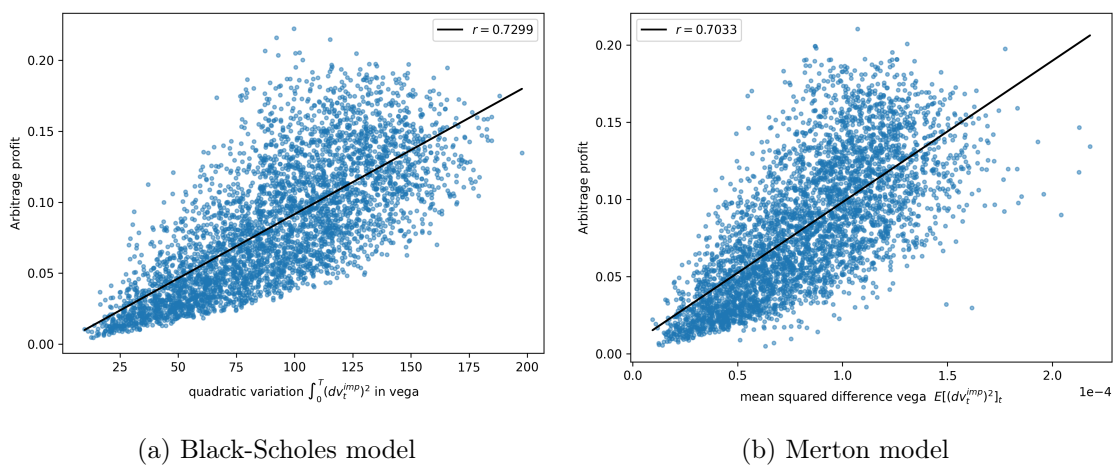


Figure 4.5: Significant Pearson correlations r are found between the random profits of the hedging strategy Δ_t^{imp} with the quadratic variations in Black-Scholes vega along the realized underlying paths.

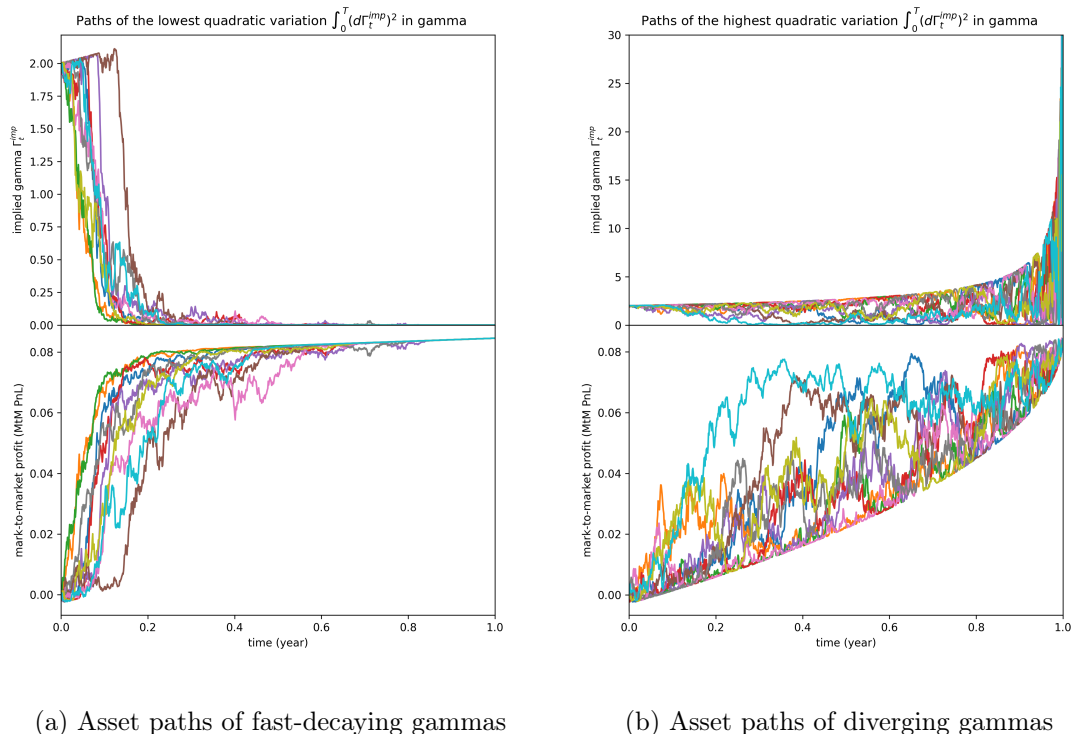


Figure 4.6: Case studies. Comparison of the mark-to-market profits of the hedging strategy Δ_t^{act} with actual volatility in the scenarios when (a) asset paths have fast-decaying gammas; versus (b) when asset paths have diverging gammas.

4.2 Part 2 Backtest of minimum variance delta-hedging

The hedging gain is presented across buckets in figure 4.7. The largest gain (30.5%) is obtained for deeply OTM call option ($\Delta_t^{BS} = 0.1$) of the 7-month maturity. The lowest gain is also obtained for call options, and is in the same Δ_t^{BS} bucket with one month maturity. Among put options, the largest gain is obtained for a similarly deeply OTM bucket ($\Delta_t^{BS} = -0.2$), also of 7-month maturity. The lowest gain (-8%) is in the ATM bucket of 1-month maturity, which likely suggests Black-Scholes' delta to be a highly effective hedge in this bucket.

For all call and put, the worst gain is attained in the near maturity bucket. Across delta buckets for this maturity, the gain is mostly negative. This could be due to the singularity $\frac{1}{\sqrt{T-t}}$ in the approximation

$$\frac{\partial E[\sigma^{imp}|G_t]}{\partial S} \approx \frac{a + b\Delta_t^{BS} + c(\Delta_t^{BS})^2}{S_t\sqrt{T-t}}$$

which reduces the sensitivity of the numerator quadratic function on the training data. The second reason could be that the Black-Scholes delta is already effective since the maturity is too short for the term structure of implied volatility to have an effect.

Between 2- to 8-month maturity, minimum variance delta mostly has good hedging performance of above 6% for deeply OTM/ITM calls, but only for deeply OTM puts.

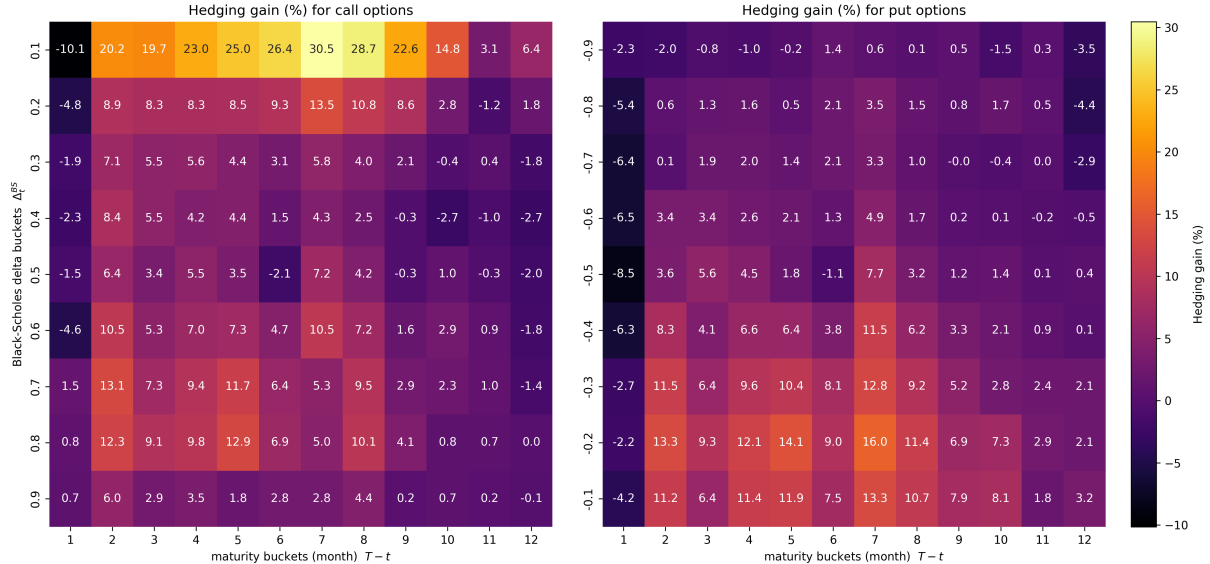


Figure 4.7: Hedging gains for call and put options over all Black-Scholes delta (Δ_t^{BS}) and maturities ($T - t$) buckets.

4.2.1 Stability and robustness

Internal model parameters (a, b, c) for a slightly in-the-money bucket of 2-month expiry are depicted in figure 4.8. This delta-maturity bucket is chosen for illustration because it has the parameter a changing sign for the call options, which reflects that the parabolic fit for predicting the expected change in implied volatility can transition to an inverted parabolic fit over time, even within the same bucket.

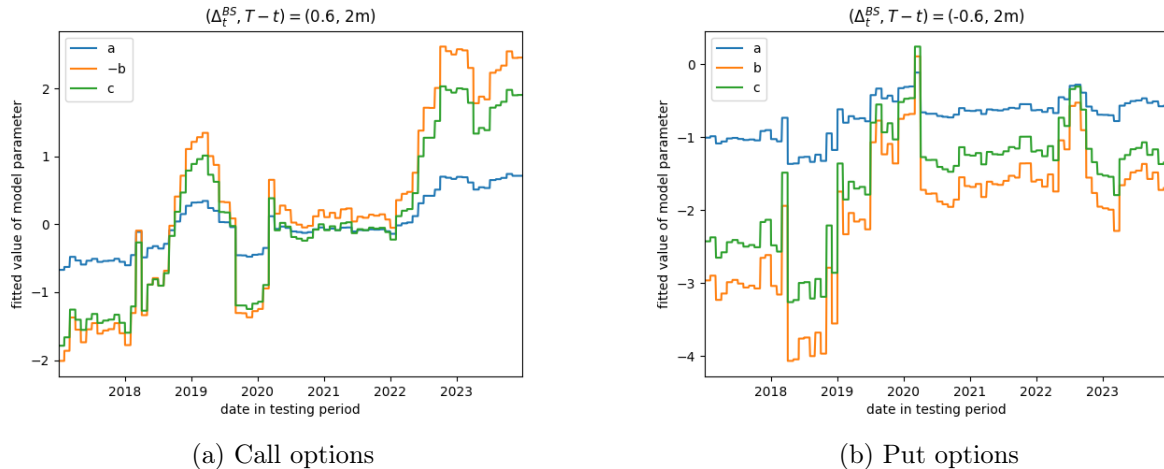


Figure 4.8: Interel model parameters (a, b, c) for a slightly in-the-money bucket of 2-month expiry.

The model parameters evolve continuously for long periods of time before exhibiting occasional large jumps, and this is true across buckets. Often, when there are large jumps observed in the fitting on call options, jumps are also observed in the fitting on put options. This suggests that some jumps result from market conditions instead of the instability of our model. There are also instances when the instability only occurs in one of the option types, and that could imply the invalidity of the assumption of quadratic fitting (or other assumptions such as the lognormal dynamics) for the market at those times.

4.2.2 Further validation

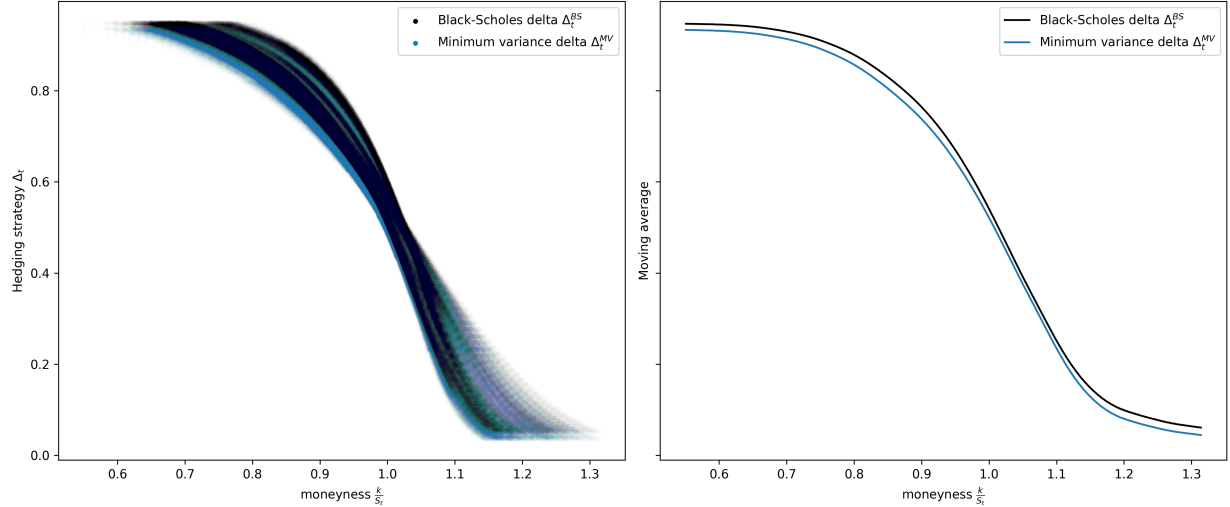
We have shown that Δ_t^{MV} has lower hedging error than Δ_t^{BS} on average. We now show that Δ_t^{MV} achieve this by under hedging call options and over hedging put options. Figure 4.9 plots the distributions of the two deltas, and moving averages are computed for each distribution for better visualization of their differences. This moving average uses a moneyness moving window of size 0.1. It is seen that across all Δ_t^{BS} levels, Δ_t^{MV} has a slightly smaller moving average in both call and put options. Note that even though the distribution span across all delta and maturity buckets, the fitting of Δ_t^{MV} is done separately for each delta-maturity bucket before being concatenated into a single distribution.

The moving average value of Δ_t^{MV} is consistently lower, but this is essentially comparing mean values and it is important to show that Δ_t^{MV} is lower on individual options. For this, the distribution of $\Delta_t^{MV} - \Delta_t^{BS}$ is shown in figure 4.10. As shown, the difference is always negative, meaning, that minimum variance delta is in fact below Black-Scholes delta for every options. $\Delta_t^{MV} - \Delta_t^{BS}$ has a quadratic shape.

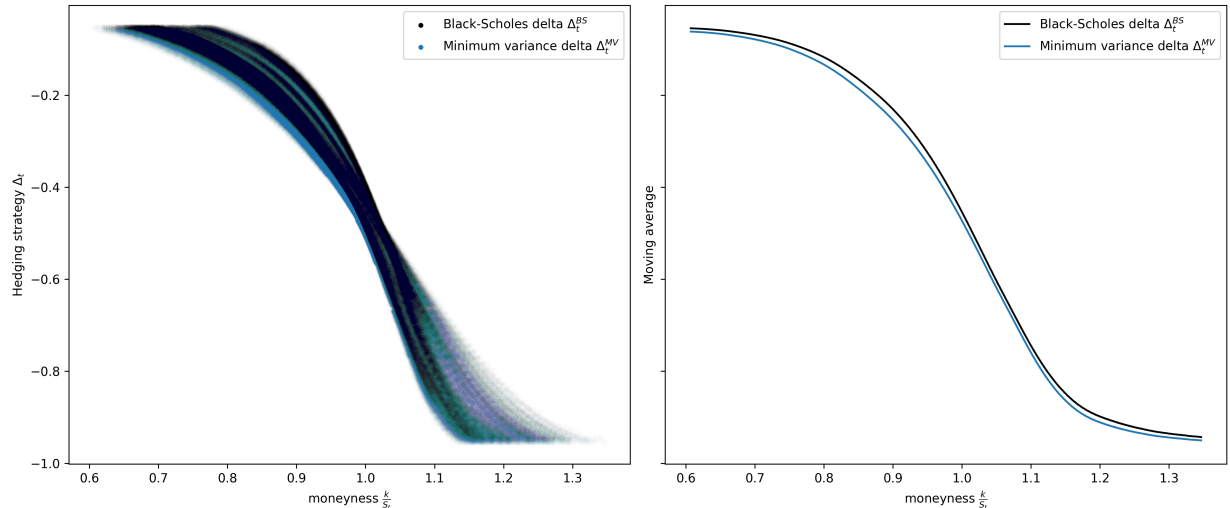
4.2.2.1 Agreement with implied volatility surface

Since vega is always positive for vanilla options, $\Delta_t^{MV} - \Delta_t^{BS} < 0$ is equivalent to $\frac{\partial E[\sigma^{imp}|G_t]}{\partial S} < 0$. The latter is confirmed in figure 4.12, with the additional finding that $\frac{\partial E[\sigma^{imp}|G_t]}{\partial S}$ decreases monotonically as option goes from OTM to ITM for maturities of 10-month or above. This is the case for both call and put options.

This agrees with what is observed in the implied volatility surfaces, that the steepest slope is attained for deeply OTM calls and puts (figure 3.4).



(a) Call options



(b) Put options

Figure 4.9: Figure shows the distributions Black-Scholes Δ_t^{BS} and minimum variance Δ_t^{MV} of every call and put options over the last 3-year fitting period. The right panels illustrate rolling averages of the deltas over moneyness. The minimum variance deltas in each moneyness-maturity bucket are obtained independently and concatenated to produce the above distributions.

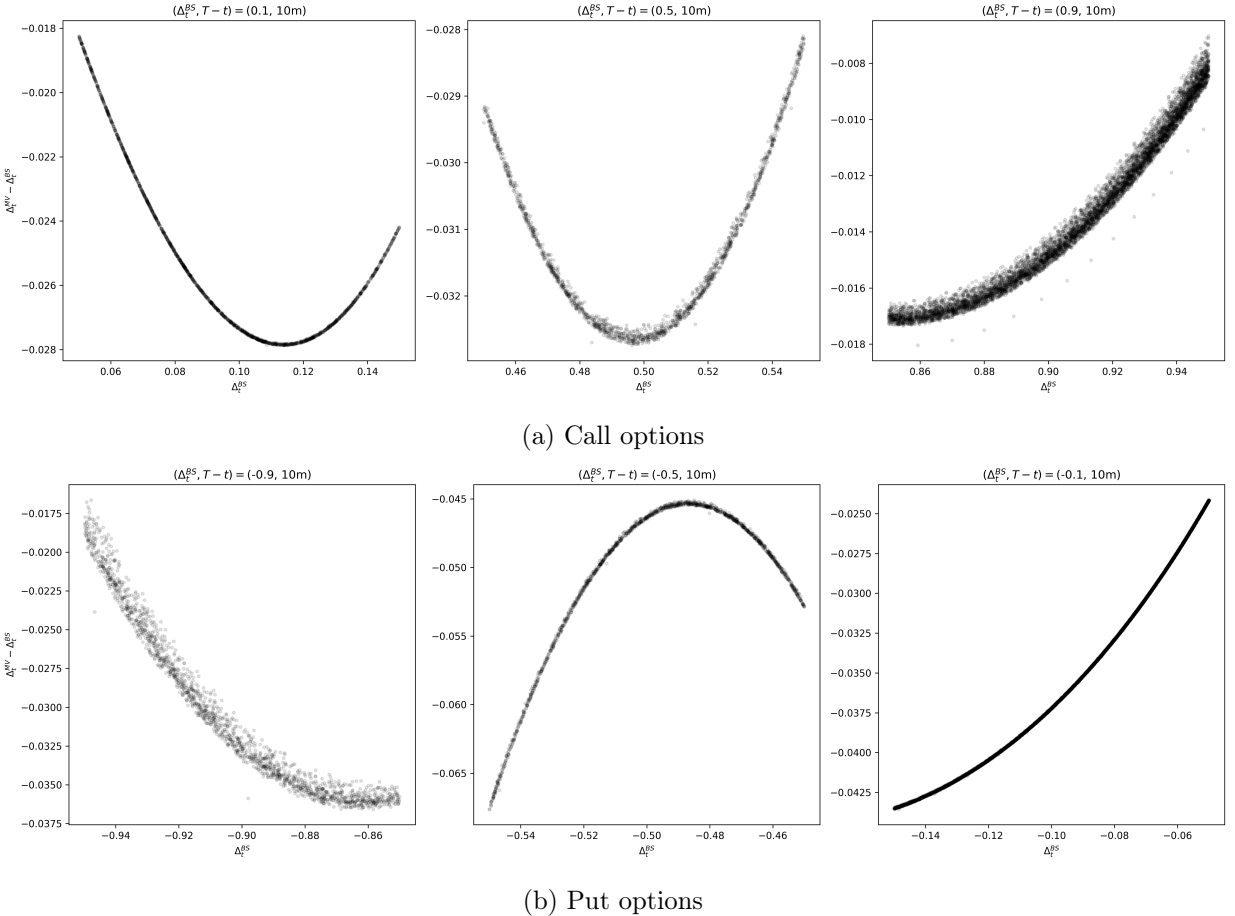


Figure 4.10: The differences between minimum variance delta Δ_t^{MV} and Black-Scholes delta Δ_t^{BS} in three Δ_t^{BS} -buckets of 10-month expiry. Delta buckets are arranged from deeply OTM, ATM, to deeply ITM for call options, and in the reverse order for put options.

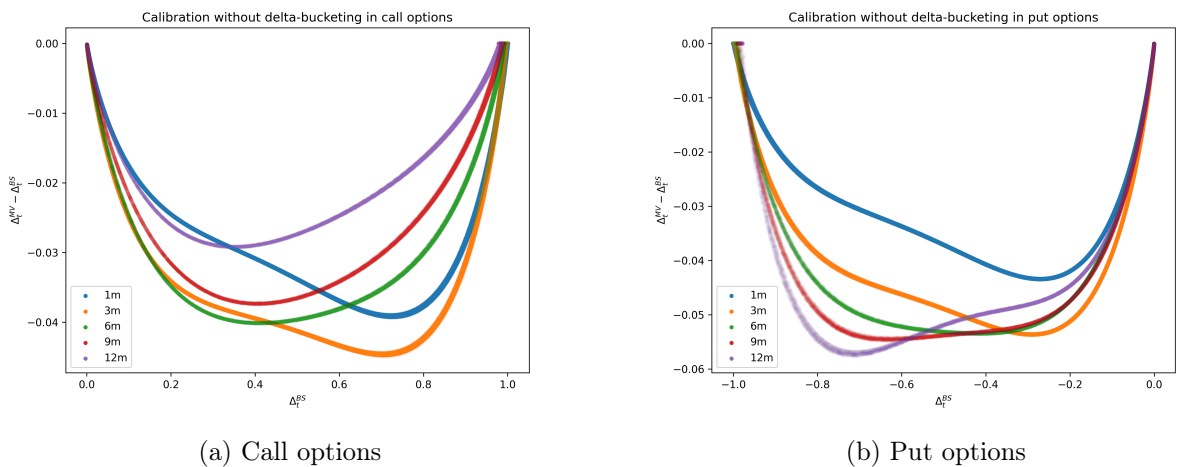


Figure 4.11: Term structure of the correct $\Delta_t^{MV} - \Delta_t^{BS}$ when the fitting is done without delta-bucketing. This is not used for backtesting but serves to give a overview of how the difference changes across maturities.

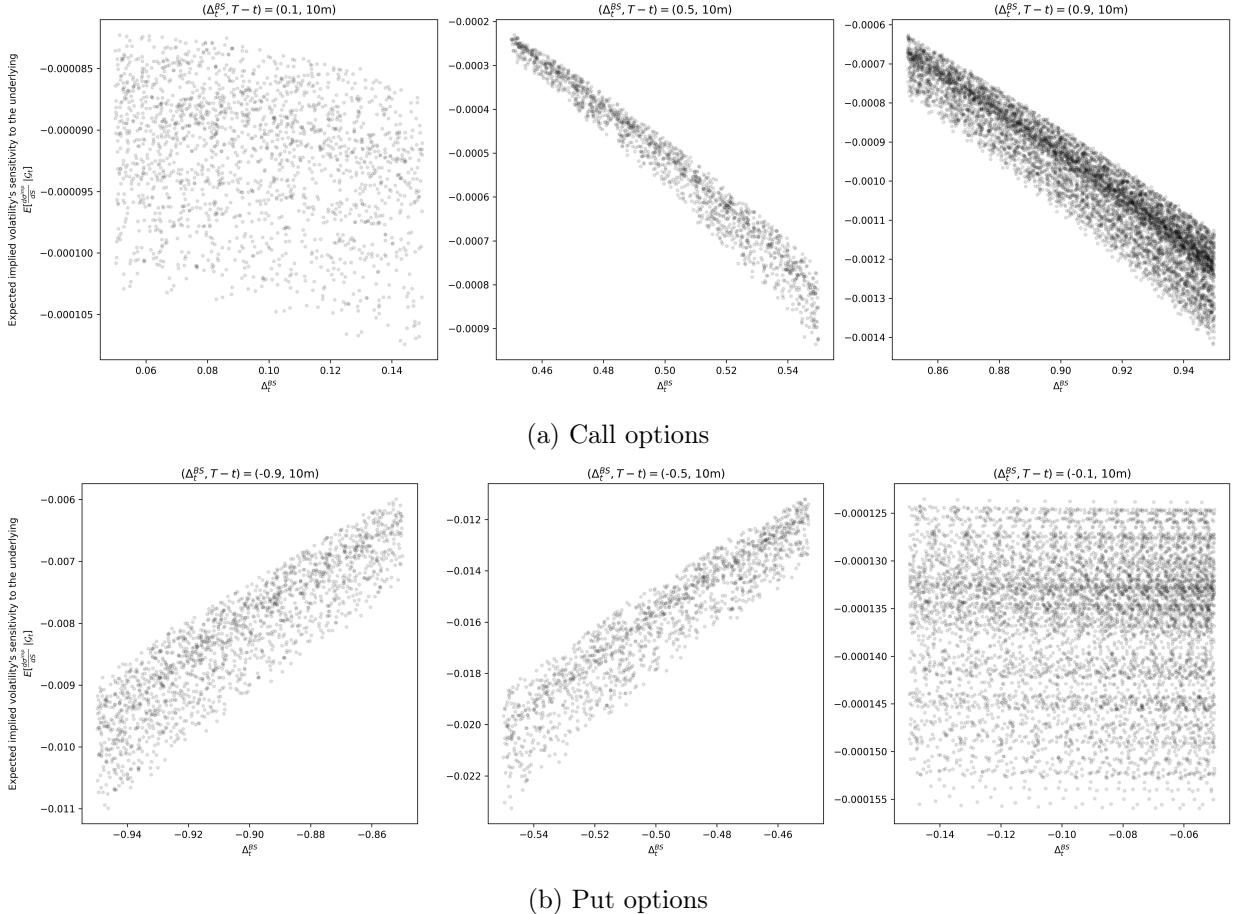


Figure 4.12: Estimators for $E[\frac{d\sigma^{imp}}{dS}(t, S_t) | \mathcal{G}_t]$ in three Δ_t^{BS} -buckets of 10-month expiry. Delta buckets are arranged from deeply OTM, ATM, to deeply ITM for call options, and in the reverse order for put options.

4.2.3 Limitations and future directions

The fact that the best performing maturity occurs at 7-month for both calls and puts may not be due to how well the quadratic fit the change in implied volatility, but could be due to there being more options at that maturity to allowing for better generalization of the fit into the testing period. Still, for the simple purpose of finding options for which the minimum variance delta hedging has an edge, so that one may focus on developing delta-hedging-reliant trading strategies in those delta-maturity buckets, the current result suffices.

The hedging strategy doesn't take into account transaction costs nor jumps in the underlying. It is shown in Part 1 that jumps has a noticeable effect on arbitrage profits if they are not hedged. It is unknown whether, when taken to real-world markets, that jumps are efficiently priced in such that not hedging them will not really affect any arbitrage profits. For future investigations, one could fit the S&P 500 with Merton's model instead, and incorporate all changes in implied volatility, jump component, and transection cost into the hedged portfolio Π_t , before minimizing the portfolio's variance. This nonetheless require the form of Δ_t^{MV} to be completely rederived, since not only would $d\Pi_t$ be different, $E[dS_t^2], E[(d\sigma_t^{imp})^2] \sim O(dt)$ would no longer hold in general.

Finally, it would be interesting to test could volatility arbitrage profits could be made by combining some volatility forecasting model with minimal variance delta-hedging. This would be a nice exercise to integrate Part 1 and 2. For example, one could use the GJR-GARCH volatility model to generate a 7-month forecast of volatility. Then, if the forecast is above the implied volatility, long call options and hedge the position with the minimum variance delta $\Delta_t^{MV} = \Delta_t^{BS,imp} + v^{BS} + t \frac{\partial E[\sigma^{imp} | \mathcal{G}_t]}{\partial S}$. Otherwise, do the reverse strategy - short the call and long a position in the underlying according to Δ_t^{MV} . Transaction costs could also be incorporated when minimizing variance, though there may no longer be a close form for Δ_t^{MV} . The final output of such backtest is expected to be a PnL for each delta-maturity bucket.

Chapter 5

Conclusion

In Part 1, this report finds that hedging with implied or actual volatility gives a slightly smaller arbitrage profits for an underlying following the Merton's model compared to one that follows that Black-Scholes model. The favourable scenarios for hedging with implied or actual volatility is then characterized in terms of the evolution in option greeks. In particular, a fast-decaying gamma ensures the early accumulation of MtM profit for hedging with actual volatility, but this is the least favourable outcome for hedging with implied volatility since the total profit is minimized. The opposite is true that a diverging gamma is the most favourable for hedging with implied volatility, but introduces huge drawdowns in the MtM profit of hedging with actual volatility. This is confirmed both numerically and analytically, and the recommendation is made to forecast gamma in addition to volatility to decide which hedging strategy to employ.

In Part 2, a maximum hedging gain of 30.5% is attained by Δ_t^{MV} for a deeply OTM call with 7-month maturity. It is found that the hedging gain is the highest also for deeply OTM put of the same maturity. The Δ_t^{MV} is found to be consistently below Δ_t^{BS} , meaning that it under hedge call options and over hedge put options relative to Black-Scholes delta. Since Black-Scholes delta reportedly over hedge ITM and OTM options, it makes sense that Δ_t^{MV} gives the largest gain on OTM calls.

Bibliography

- [1] John C. Hull and Alan White. “Optimal Delta Hedging for Options”. In: *Journal of Banking and Finance* 82 (Sept. 2017), pp. 180–190. DOI: [10.2139/ssrn.2658343](https://doi.org/10.2139/ssrn.2658343). eprint: <https://ssrn.com/abstract=2658343>. URL: <https://ssrn.com/abstract=2658343>.
- [2] Robert C. Merton. “Option pricing when underlying stock returns are discontinuous”. In: *Journal of Financial Economics* 3.1 (1976), pp. 125–144. ISSN: 0304-405X. DOI: [https://doi.org/10.1016/0304-405X\(76\)90022-2](https://doi.org/10.1016/0304-405X(76)90022-2). URL: <https://www.sciencedirect.com/science/article/pii/0304405X76900222>.
- [3] Michael B. Giles and Ben J. Waterhouse. “Multilevel Quasi-Monte Carlo Path Simulation”. In: *Radon Series on Computational and Applied Mathematics* 8 (2009), pp. 1–18. DOI: [10.1515/9783110218053.1](https://doi.org/10.1515/9783110218053.1). eprint: <https://people.maths.ox.ac.uk/gilesm/files/radon.pdf>. URL: <https://people.maths.ox.ac.uk/gilesm/files/radon.pdf>.
- [4] OptionMetrics. *IvyDB US: Historical Option Price and Implied Volatility Data*. OptionMetrics, Accessed 2025. URL: <https://optionmetrics.com>.
- [5] Benjamin Golez and Jens Carsten Jackwerth. “Holding Period Effects in Dividend Strip Returns”. In: *SSRN Electronic Journal* (Nov. 2023). DOI: [10.2139/ssrn.4015723](https://doi.org/10.2139/ssrn.4015723). eprint: <https://ssrn.com/abstract=4015723>. URL: <https://ssrn.com/abstract=4015723>.
- [6] Muoria Kamau and Ivivi J. Mwaniki. “On a robust estimation of option-implied interest rates and dividend yields”. In: *Cogent Economics & Finance* 11.2 (2023), p. 2260658. DOI: [10.1080/23322039.2023.2260658](https://doi.org/10.1080/23322039.2023.2260658). eprint: <https://doi.org/10.1080/23322039.2023.2260658>. URL: <https://doi.org/10.1080/23322039.2023.2260658>.